

Crystal Structure and Electrical Conductivity of Mixed Conductive $\text{BaIn}_{1-x}\text{M}_x\text{O}_{3-\delta}$ (M = Ti, V, Cr, Mn, Fe, Co, Ni, or Cu)

Teruaki Kobayashi, Akifumi Hasesaka, Mitsuhiro Hibino, Takeshi Yao

Graduate School of Energy Science, Kyoto University, Sakyo-ku, Kyoto, 606-8501

Fax: +81-75-753-4735, e-mail: teruaki.k@t01.mbox.media.kyoto-u.ac.jp

For development of mixed conductors, we synthesized $\text{BaIn}_{1-x}\text{M}_x\text{O}_{3-\delta}$ (M = Ti, V, Cr, Mn, Fe, Co, Ni, or Cu) by substitution of transition metals for indium. The $\text{BaIn}_{1-x}\text{M}_x\text{O}_{3-\delta}$ has orthorhombic, tetragonal or cubic structure depending on the kind and amount of the transition metals at room temperature. The structural transition temperatures from orthorhombic to a higher symmetric structure decreased with substitution for indium. For the samples with cubic perovskite structures at room temperature, no structural transition was observed from room temperature to 1000 °C. $\text{BaIn}_{0.8}\text{Fe}_{0.2}\text{O}_{3-\delta}$ and $\text{BaIn}_{0.8}\text{Co}_{0.2}\text{O}_{3-\delta}$ showed higher conductivity than $\text{Ba}_2\text{In}_2\text{O}_5$ and showed no steep change in conductivity with temperature. Hole as well as oxide ion was responsible for their high electrical conductivity since their conductivity versus oxygen partial pressure exhibited typical behavior in p-type electronic conduction. Consequently, they are expected to be favorable mixed conductors.

Key words: Barium indium oxide, Perovskite structure, Mixed conduction, Charge carrier

1. INTRODUCTION

Oxide ionic and electronic mixed conductive materials have potential for active catalysts in gas-solid reactions and expected to serve as electrodes of solid oxide fuel cells (SOFCs), oxygen permeating membranes, gas sensors, membrane reactors and etc. In recent years, some researchers and our group have synthesized mixed conductors derived from an oxide ionic conductor by substitution of a transition metal [1 – 6].

Barium indium oxide ($\text{Ba}_2\text{In}_2\text{O}_5$) shows a high oxide ionic conductivity via oxygen vacancies above approximately 930 °C [7]. However, the structural transition from a high temperature perovskite type to a low temperature brownmillerite one dramatically reduces its conductivity because oxygen vacancies are in rows along [101] directions of the perovskite structure at low temperatures. It has been clarified that partial substitution of lanthanum, gallium or gadolinium for barium or indium lowers the transition temperature, and retains oxide ionic conductivity even at low temperatures [8 – 11]. Some of them show higher oxide ionic conductivity than the high-temperature phase of the original $\text{Ba}_2\text{In}_2\text{O}_5$ and they have been applied to SOFCs [12 – 14].

In our previous study, $\text{BaIn}_{1-x}\text{Co}_x\text{O}_{3-\delta}$ was synthesized by partial substitution of cobalt for indium in $\text{Ba}_2\text{In}_2\text{O}_5$ for production of a mixed conductor. $\text{BaIn}_{1-x}\text{Co}_x\text{O}_{3-\delta}$ was a cubic perovskite structure and retained oxide ionic conduction even at low temperature. At the same time, electronic conduction emerged by the introduction of mixed valence state of cobalt. A mixed conductive $\text{BaIn}_{1-x}\text{Co}_x\text{O}_{3-\delta}$ was prepared successfully [6]. In the present paper, we attempt to synthesize a series of $\text{BaIn}_{1-x}\text{M}_x\text{O}_{3-\delta}$ (M = Ti, V, Cr, Mn, Fe, Co, Ni, or Cu) in which indium is replaced partially by transition metals in the fourth period, and discuss their

crystal structures and electrical conductivity, especially in terms of charge carriers.

2. EXPERIMENTAL

Barium carbonate and indium oxide were mixed with the oxide, hydroxide, or carbonate of a required transition metal in various ratios, and ground in an electric mortar with a pestle. The mixture was pressed into a disk, and heated in air at various temperatures ranging from 950 to 1350 °C depending on the kind and amount of the added transition metal. The product was ground and analyzed by powder X-ray diffractometry (XRD) with $\text{CuK}\alpha$ radiation at room temperature. Then, the product powder was shaped into a disk, and pressed by a cold isostatic press at 392 MPa. The disk was sintered under the temperature same as that in the former thermal treatment. The product thus sintered was cut into a rectangular prism $4 \times 10 \times 2 \text{ mm}^3$ in size for the measurement of electrical conductivity.

For the determination of the structural transition temperature, differential scanning calorimetry (DSC) was performed in air between room temperature and 1200 °C at $10 \text{ }^\circ\text{C min}^{-1}$ of the heating or cooling rates.

The electrical conductivity was measured by DC four-probe method in the range 600 – 1000 °C. Oxygen partial pressure (P_{O_2}) was controlled from 10^2 to 10^5 Pa by a regulation of ratio of $\text{Ar}/\text{N}_2/\text{O}_2$.

3. RESULTS AND DISCUSSION

3.1 Characterization

Crystal systems for $\text{BaIn}_{1-x}\text{M}_x\text{O}_{3-\delta}$ (M = Ti, V, Cr, Mn, Fe, Co, Ni, or Cu) determined by XRD at room temperature are shown in Fig.1. The samples indicated by filled circles have cubic perovskite structures. Neither peak nor baseline step in DSC charts (not shown here) was observed for these samples, indicating that no structural transition occurred. Therefore, high oxide

ionic conductivity was expected in these samples because oxygen vacancies were suggested to be distributed randomly. The samples with tetragonal structures are shown by open circles. The DSCs for these samples showed no structural transition except for $BaIn_{0.8}Co_{0.2}O_{3-\delta}$. This suggested that the samples except for $BaIn_{0.8}Co_{0.2}O_{3-\delta}$ underwent no structural transition at temperatures below 1200 °C. DSC for $BaIn_{0.8}Co_{0.2}O_{3-\delta}$ implies structural transition around 750 °C. This was due to disappearance and appearance of superstructure [6]. Filled squares show the samples with orthorhombic brownmillerite structures. For these samples, exothermal peaks were observed in the heating process of DSC, indicating that the transformation from orthorhombic to tetragonal structures. The relevant endothermal ones in the cooling process were also observed. The samples shown by open squares were mixtures of two or more phases.

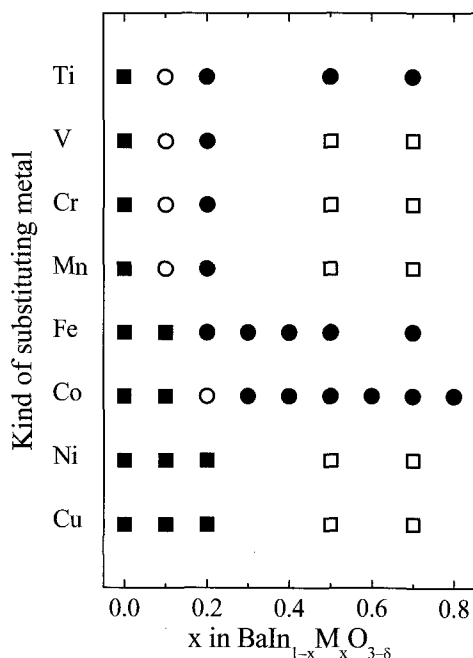


Fig.1 Crystal systems of $BaIn_{1-x}M_xO_{3-\delta}$ at room temperature determined by XRD profiles. Filled circles, open circles and filled squares indicate the sample with cubic, tetragonal and orthorhombic structures, respectively. Mixture or unidentified samples were indicated by open squares.

3.2 Electrical Properties

Figure 2 shows electrical conductivities of $Ba_2In_2O_5$ and $BaIn_{0.8}M_{0.2}O_{3-\delta}$ ($M = Ti, V, Cr, Mn, Fe, Co, Ni, \text{ or } Cu$) versus reciprocal temperatures in air. The conductivity of $Ba_2In_2O_5$ changed steeply between 950

and 900 °C due to the transformation between tetragonal and orthorhombic systems. The electrical conductivities of $BaIn_{0.8}M_{0.2}O_{3-\delta}$ ($M = Ti, V, Cr, Mn, Ni, \text{ or } Cu$) showed no such abrupt change and were higher than that of $Ba_2In_2O_5$ at low temperature. In contrast, the conductivity of these samples was lower than that of $Ba_2In_2O_5$ at high temperature. The electrical conductivity of $BaIn_{0.8}Fe_{0.2}O_{3-\delta}$ and $BaIn_{0.8}Co_{0.2}O_{3-\delta}$ also showed no abrupt change, and was higher than that of the high temperature phase of $Ba_2In_2O_5$. For $BaIn_{0.8}Co_{0.2}O_{3-\delta}$, a discontinuous change was observed between 850 and 800 °C though the gap was small. This temperature was close to that of the DSC peaks described above. Hence, electrical conductivity of $BaIn_{0.8}Co_{0.2}O_{3-\delta}$ seemed to change in response to the superlattice formation.

The apparent activation energies of electrical conductivity are listed in Table I. The activation energies for $BaIn_{0.8}M_{0.2}O_{3-\delta}$ ($M = Ti, V, Cr, Mn, Fe, Co, Ni, \text{ or } Cu$) were lower than that of the original $Ba_2In_2O_5$. This implies that the charge carriers different from oxide ion contributed to total electrical conductivity.

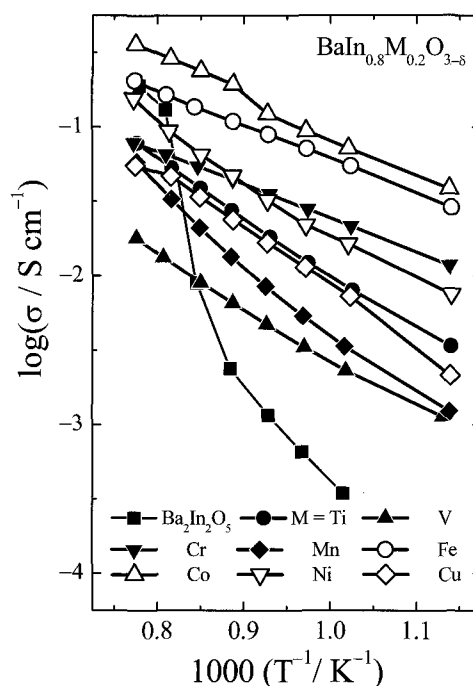


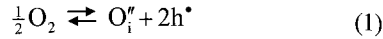
Fig.2 Arrhenius plots of total electrical conductivities for $BaIn_{0.8}M_{0.2}O_{3-\delta}$ in air.

Table I Apparent activation energies for the electrical conduction of $BaIn_{0.8}M_{0.2}O_{3-\delta}$ estimated at 925 °C.

Apparent activation energy / kJ mol^{-1}	$Ba_2In_2O_5$	$BaIn_{0.8}M_{0.2}O_{3-\delta}$							
		M = Ti	V	Cr	Mn	Fe	Co	Ni	Cu
	*112.3	81.2	74.1	52.2	107.6	52.6	55.9	93.5	**86.6

*Estimated at 975 °C, **Estimated at 900 °C

The electrical conductivities of $Ba_2In_2O_5$ and $BaIn_{0.8}M_{0.2}O_{3-\delta}$ ($M = Ti, V, Cr, Mn, Fe, Co, Ni, \text{ or } Cu$) as a function of P_{O_2} at 850 °C is shown in Fig.3. The electrical conductivity of $Ba_2In_2O_5$ was proportional to $P_{O_2}^{1/6}$ at 850 °C, which was lower than the transition temperature. In the brownmillerite oxide, oxide ion is induced according to the following chemical equation (1) using Kröger-Vink notation.



Equilibrium constant for equation (1) is described by equation (2).

$$K_{ox} = [O_i''] [h^\bullet]^2 P_{O_2}^{-1/2} \quad (2)$$

Considering charge neutrality condition, the hole concentration is described by equation (3).

$$[h^\bullet] = (2K_{ox})^{1/2} P_{O_2}^{1/6} \quad (3)$$

The result of electrical conductivity for $Ba_2In_2O_5$ at 850 °C agreed well with equation (3). This indicates that the dominant charge carrier was hole in the low temperature phase of $Ba_2In_2O_5$, and agreed well with the result reported by Zhang et al. [15].

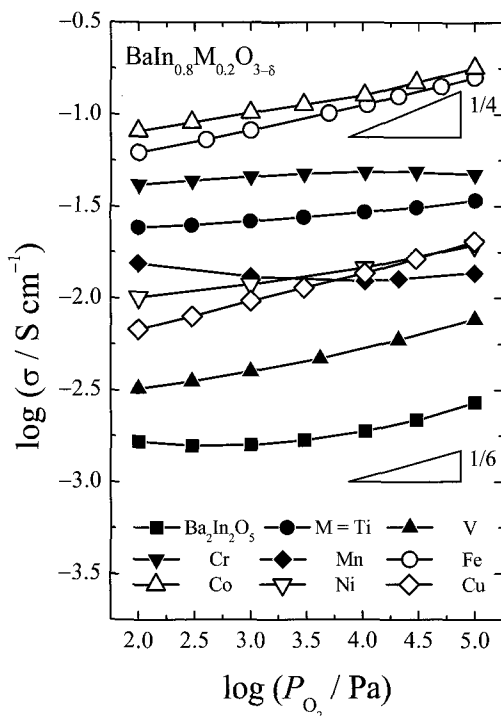
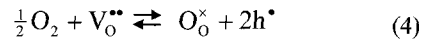


Fig.3 Electrical conductivity of $BaIn_{1-x}M_xO_{3-\delta}$ against oxygen partial pressure at 850 °C.

The logarithm of electrical conductivities ($\log \sigma$) for $BaIn_{0.8}M_{0.2}O_{3-\delta}$ ($M = V, Fe, Co, Ni, \text{ or } Cu$) showed positive slopes versus logarithm of P_{O_2} ($\log P_{O_2}$). In a defective perovskite oxide, oxide ion is induced

according to equation (4).



Equilibrium constant for equation (4) is described by equation (5).

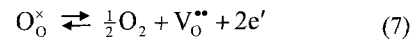
$$K_{ox} = [V_O^{\bullet\bullet}]^{-1} [h^\bullet]^2 P_{O_2}^{-1/2} \quad (5)$$

Then the hole concentration is described by equation (6).

$$[h^\bullet] = (K_{ox} [V_O^{\bullet\bullet}])^{1/2} P_{O_2}^{1/4} \quad (6)$$

According to equation (6), the hole concentration is proportional to $P_{O_2}^{1/4}$. The positive slopes of $\log \sigma$ versus $\log P_{O_2}$ for $BaIn_{0.8}M_{0.2}O_{3-\delta}$ ($M = V, Fe, Co, Ni, \text{ or } Cu$) indicate p-type electronic conduction though they are less than 1/4. This suggests mixed conduction of oxide ion and hole. On the other hand, $BaIn_{0.8}M_{0.2}O_{3-\delta}$ ($M = Ti \text{ or } Cr$) showed small degree of dependence of conductivity on the oxygen pressure while it also showed the p-type conduction behavior. This result suggests that ionic conduction contributed significantly to total electrical conduction in $BaIn_{0.8}M_{0.2}O_{3-\delta}$ ($M = Ti \text{ or } Cr$).

The slope of $\log \sigma$ for $BaIn_{0.8}Mn_{0.2}O_{3-\delta}$ was negative versus $\log P_{O_2}$. Oxide ion can be extracted from perovskite oxides according to the following equation (7).



Equilibrium constant for equation (7) is described by equation (8).

$$K_{red} = [V_O^{\bullet\bullet}] [e']^2 P_{O_2}^{-1/2} \quad (8)$$

Then the electron concentration is described by equation (9).

$$[e'] = (K_{red} [V_O^{\bullet\bullet}]^{-1})^{1/2} P_{O_2}^{-1/4} \quad (9)$$

According to equation (9), the electron concentration is proportional to $P_{O_2}^{-1/4}$. The negative slope of $\log \sigma$ versus $\log P_{O_2}$ for $BaIn_{0.8}Mn_{0.2}O_{3-\delta}$ indicates n-type electronic conduction while it is more than -1/4 (the absolute value of the slope is less than 1/4).

The electrical conductivities of $Ba_2In_2O_5$ and $BaIn_{0.8}M_{0.2}O_{3-\delta}$ ($M = Ti, V, Cr, Mn, Fe, Co, Ni, \text{ or } Cu$) as a function of P_{O_2} at 1000 °C is shown in Fig.4. The electrical conductivity of $Ba_2In_2O_5$ is independent of the P_{O_2} . This indicates that the dominant charge carrier was oxide ion in the high temperature phase of $Ba_2In_2O_5$, and agreed well with the result reported by Zhang et al. [15]. The $\log \sigma$ for $BaIn_{0.8}M_{0.2}O_{3-\delta}$ ($M = Ti, V, Cr, Fe, Co, Ni, \text{ or } Cu$) showed positive slope versus $\log P_{O_2}$. This indicates that p-type conduction contributed to total electrical conductivity. In contrast, $BaIn_{0.8}Mn_{0.2}O_{3-\delta}$ showed a negative slope versus $\log P_{O_2}$, indicating a contribution of n-type conduction.

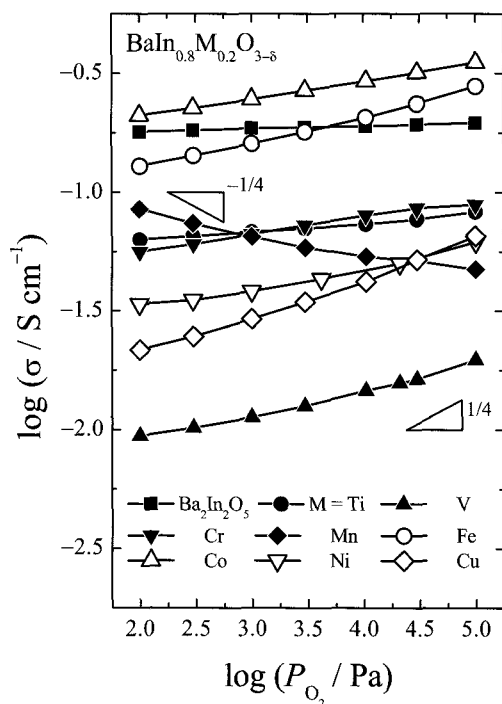


Fig.4 Electrical conductivity of $BaIn_{1-x}M_xO_{3-\delta}$ against oxygen partial pressure at 1000 °C.

4. SUMMARY

The crystal structure and transition behavior of $BaIn_{1-x}M_xO_{3-\delta}$ ($M = Ti, V, Cr, Mn, Fe, Co, Ni, \text{ or } Cu$) were investigated by XRD and DSC, respectively. $BaIn_{1-x}M_xO_{3-\delta}$ ($M = Ti, V, Cr, Mn, Fe, Co, Ni, \text{ or } Cu$) had cubic, tetragonal or orthorhombic structures depending on the kind and the amount of transition metals. Partial substitution of Ti, V, Cr, Mn, Fe, or Co for indium was found to be effective to stabilize cubic perovskite structure at low temperature. For the samples with orthorhombic structures, the transition temperatures from orthorhombic to tetragonal were reduced. As a result, $BaIn_{1-x}M_xO_{3-\delta}$ ($M = Ti, Fe, \text{ or } Co$) was in the cubic system at room temperature.

The electrical conductivities of $BaIn_{0.8}M_{0.2}O_{3-\delta}$ were measured as a function of temperature and P_{O_2} . $BaIn_{0.8}Fe_{0.2}O_{3-\delta}$ and $BaIn_{0.8}Co_{0.2}O_{3-\delta}$ showed higher electrical conductivities than the high temperature phase of the original $Ba_2In_2O_5$. Since their conductivity against P_{O_2} exhibited typical behavior in p-type electronic conduction, hole as well as oxide ion was responsible for their high electrical conductivity. Consequently, they are expected to be favorable mixed conductors.

NOMENCLATURE

P_{O_2} = oxygen partial pressure [Pa]

K = equilibrium constant

[X] = concentration of X in oxide [mol-X / mol-perovskite]

σ = electrical conductivity [$S\ cm^{-1}$]

ACKNOWLEDGEMENTS

One of the authors, T. K., thanks Japan Society for the Promotion of Science (JSPS) for financial support to a research fellow. This work was partly supported by a Grant-in-Aid for JSPS Fellows by JSPS.

REFERENCES

- [1] T. Kawada, N. Sakai, H. Yokokawa, M. Dokiya, *Solid State Ionics*, **53-56**, 418-25 (1992).
- [2] F. Chen, M. Liu, *J. Solid State Electrochem.*, **3**, 7-14 (1998).
- [3] Y. Aizumi, H. Takamura, A. Kamegawa, M. Okada, *J. Ceram. Soc. Jpn.*, **112**, S724-28 (2004).
- [4] K. Kakinuma, K. Yamakawa, S. Hasunuma, H. Yamamura, T. Atake, *Solid State Ionics*, **177**, 1317-22 (2006).
- [5] D. P. Fagg, J. R. Frade, V. V. Kharton, I. P. Marozau, *J. Solid State Chem.*, **179**, 1469-77 (2006).
- [6] T. Kobayashi, Y. Senoo, M. Hibino, T. Yao, *Solid State Ionics*, **177**, 1743-46 (2006).
- [7] J. B. Goodenough, J. E. Ruiz-Diaz, Y. S. Zhen, *Solid State Ionics*, **44**, 21-31 (1990).
- [8] Y. Uchimoto, T. Yao, H. Takagi, T. Inagaki, H. Yoshida, *Electrochemistry*, **68**, 531-3 (2000).
- [9] K. Kakinuma, H. Yamamura, H. Haneda, T. Atake, *Solid State Ionics*, **140**, 301-06 (2001).
- [10] T. Yao, Y. Uchimoto, M. Kinuhata, T. Inagaki, H. Yoshida, *Solid State Ionics*, **132**, 189-98 (2000).
- [11] Y. Uchimoto, M. Kinuhata, T. Yao, *Jpn. J. Appl. Phys.*, **38**, 111-14 (1999).
- [12] K. Kakinuma, T. Arisaka, H. Yamamura, T. Atake, *Solid State Ionics*, **175**, 139-43 (2004).
- [13] S. Asahara, D. Michiba, M. Hibino, T. Yao, *Electrochemical and Solid State Letters*, **8**, A449-51 (2005).
- [14] M. Hibino, D. Michiba, K. Kanatani, H. Suzuki, T. Yao, *Advances in Science and Technology*, **45**, 1875-1878 (2006).
- [15] G. B. Zhang, D. M. Smyth, *Solid State Ionics*, **82**, 161-72 (1995).

(Received December 9, 2007 ; Accepted September 1, 2008)